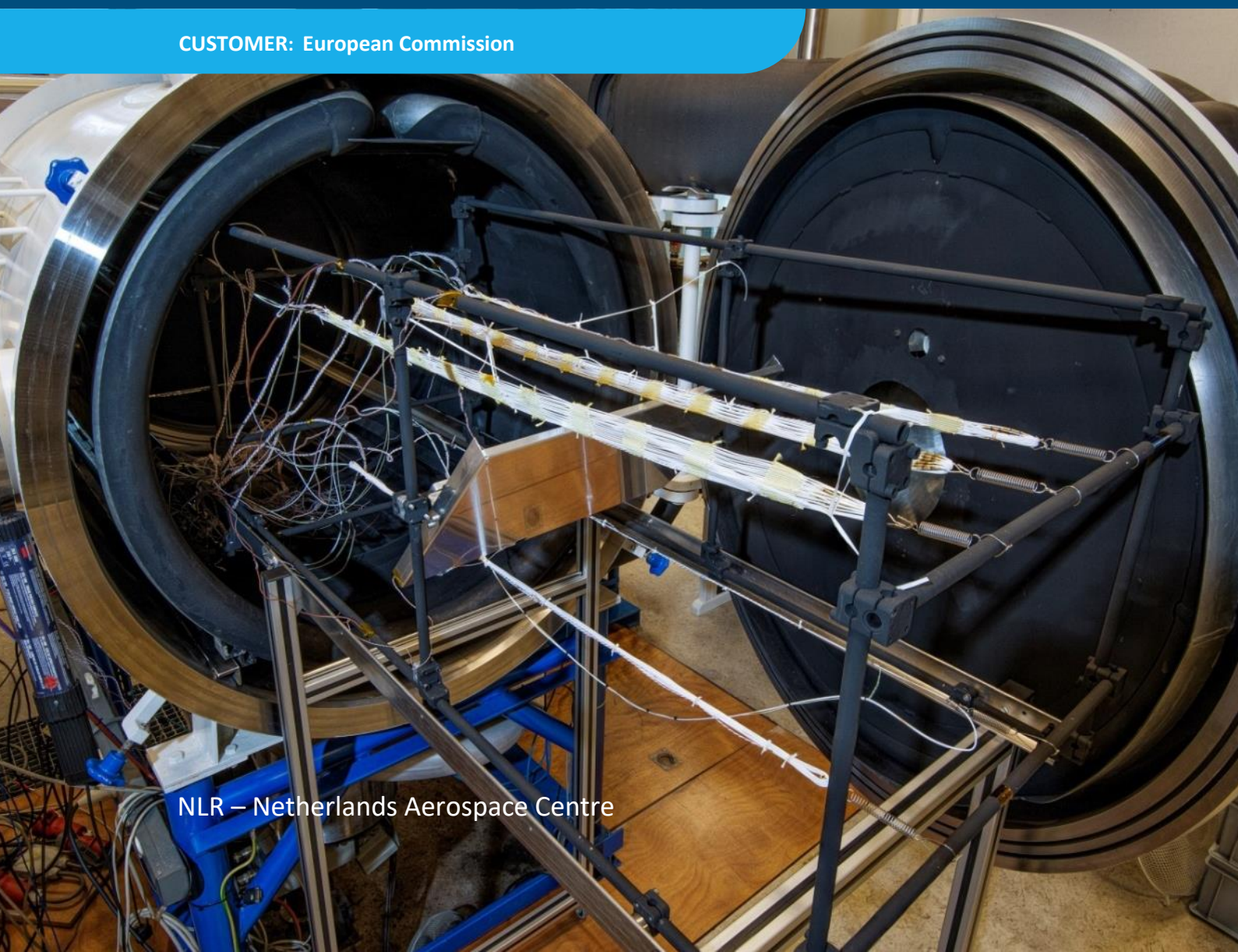


# Flat cable derating tests and thermal modelling for weight reduction of aircraft engine harness designs

CUSTOMER: European Commission



## Netherlands Aerospace Centre

NLR is a leading international research centre for aerospace. Bolstered by its multidisciplinary expertise and unrivalled research facilities, NLR provides innovative and integral solutions for the complex challenges in the aerospace sector.

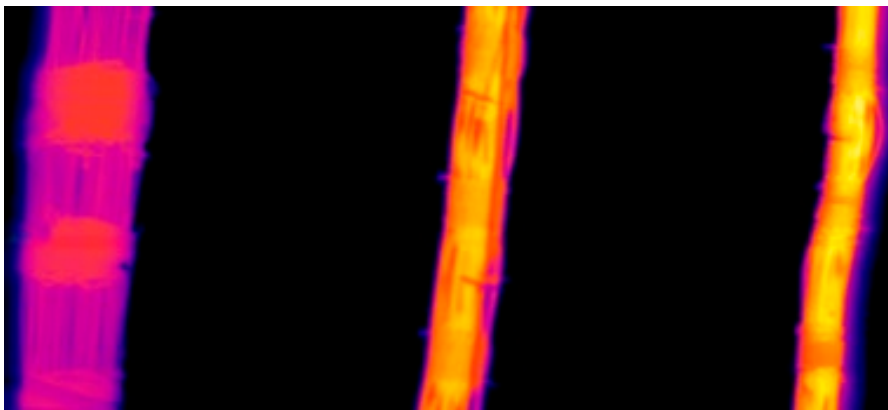
NLR's activities span the full spectrum of Research Development Test & Evaluation (RDT & E). Given NLR's specialist knowledge and facilities, companies turn to NLR for validation, verification, qualification, simulation and evaluation. NLR thereby bridges the gap between research and practical applications, while working for both government and industry at home and abroad.

NLR stands for practical and innovative solutions, technical expertise and a long-term design vision. This allows NLR's cutting edge technology to find its way into successful aerospace programs of OEMs, including Airbus, Embraer and Pilatus. NLR contributes to (military) programs, such as ESA's IXV re-entry vehicle, the F-35, the Apache helicopter, and European programs, including SESAR and Clean Sky 2.

Founded in 1919, and employing some 600 people, NLR achieved a turnover of 76 million euros in 2017, of which 81% derived from contract research, and the remaining from government funds.

For more information visit: [www.nlr.nl](http://www.nlr.nl)

# Flat cable derating tests and thermal modelling for weight reduction of aircraft engine harness designs



## Problem area

With the development of new turbofan aero engines, such as the Ultra-High Bypass Ratio (UHBR) engine and open-rotor solutions, advances in propulsion and fuel efficiency can be made through increasing fan diameters and higher bypass-ratios. This will provide less space for the engine systems and for ventilation. Moreover, higher operating temperatures are being expected. Improved technologies for the more severe conditions were investigated in the EU H2020 research project NIPSE. One of the objectives was to assess innovative flat-cable designs for extreme environmental conditions that occur in nacelles. Since flat cables have a larger cooling surface than round bundles, the derating of flat cables is expected to be less severe with respect to the recommended industrial derating in AS50881 for round bundles designs. As a consequence smaller wire gauges may be allowed in flat cables when compared to round bundles while carrying the same current, thus saving weight.

## Description of work

To investigate this, three experimental flat cable samples (1, 2, and 3 layers of in total 22 AWG 20) have been manufactured and tested in horizontal as well as in 90 degrees rotated orientation together with references samples. The innovative

### REPORT NUMBER

NLR-TP-2019-040

### AUTHOR(S)

R.C. van Benthem  
E.A. Bloem  
F. Alberio  
L. Azemard

### REPORT CLASSIFICATION

UNCLASSIFIED

### DATE

August 2019

### KNOWLEDGE AREA(S)

Electronics Technology  
Avionics Qualification

### DESCRIPTOR(S)

Flat cable  
Thermal derating  
standards  
Thermal Modeling  
Weight Saving

derating tests, done in an altitude chamber, showed an improved performance compared to the standard AS50881 derating, demonstrating the weight saving potential of flat cables.

## Results and conclusions

The test results show that the derating of flat cables should be related to the number of layers. The main trend for a 1 layer flat cable shows an increased current capability (at the same temperature differences) which can lead to a significant weight reduction up to 60%. Future investigation on use cases is required to substantiate this. Thermal modelling has been done for correlation with the derating test results and for extrapolation toward higher environmental temperature conditions up to 240°C as found in aircraft engines. The analysis indicated a model accuracy of  $\pm 5.95^{\circ}\text{C}$ . Future investigation to improve flat cable manufacturing methods and derating testing is recommended for optimization and use of flat cable designs by the aircraft industry in general.

## Applicability

This research will pave the way for an extension and improvement of the aerospace derating standards allowing the use of flat cables, saving weight, easing installation in narrow areas, and improving fuel economy for new aircraft.

### GENERAL NOTE

This report is based on a presentation held at the AEGATS 2018 conference, Toulouse, France, 23-25 October 2018.

### NLR

Anthony Fokkerweg 2

1059 CM Amsterdam

p ) +31 88 511 3113

e ) [info@nlr.nl](mailto:info@nlr.nl) i ) [www.nlr.nl](http://www.nlr.nl)



Dedicated to innovation in aerospace

NLR-TP-2019-040 | August 2019

# Flat cable derating tests and thermal modelling for weight reduction of aircraft engine harness designs

CUSTOMER: European Commission

## AUTHOR(S):

R.C. van Benthem

E.A. Bloem

F. Albero

L. Azemard

NLR

NLR

SAFRAN ELECTRICAL & POWER

SAFRAN ELECTRICAL & POWER

This report is based on a presentation held at the AEGATS 2018 conference, Toulouse, France, 23-25 October 2018.

*The contents of this report may be cited on condition that full credit is given to NLR and the author.*

<b>CUSTOMER</b>	European Commission
<b>CONTRACT NUMBER</b>	636218
<b>OWNER</b>	NLR + partner(s)
<b>DIVISION NLR</b>	Aerospace Systems
<b>DISTRIBUTION</b>	Unlimited
<b>CLASSIFICATION OF TITLE</b>	UNCLASSIFIED

APPROVED BY :		
AUTHOR	REVIEWER	MANAGING DEPARTMENT
R.C. van Benthem	E.A. Bloem	T. Slijkerman
DATE	DATE	DATE

# Contents

<b>Abbreviations</b>	<b>4</b>
<b>Abstract</b>	<b>5</b>
<b>1 Introduction</b>	<b>5</b>
<b>2 Flat cable derating tests</b>	<b>6</b>
<b>3 Tested samples</b>	<b>7</b>
<b>4 Test sequence</b>	<b>9</b>
<b>5 IR camera measurements</b>	<b>9</b>
<b>6 Temperature measurements</b>	<b>9</b>
<b>7 Derating evaluation approach</b>	<b>10</b>
<b>8 Derating results</b>	<b>11</b>
<b>9 Thermal modelling</b>	<b>13</b>
<b>10 Conclusions &amp; recommendations</b>	<b>14</b>
<b>11 Acknowledgements</b>	<b>14</b>
<b>References</b>	<b>14</b>

## Abbreviations

ACRONYM	DESCRIPTION
AWG	American Wire Gauge
ECSS	European Cooperation for Space Standardization
ESA	European Space Agency
HDTF	Harness Derating Test Facility
IR	Infrared
NIPSE	Novel Integration of Powerplant System Equipment
NLR	Netherlands Aerospace Centre
SEP	SAFRAN Electric & Power
TC	Thermocouple
TV	Thermal Vacuum
UHBR	Ultra-High Bypass Ratio



# FLAT CABLE DERATING TESTS AND THERMAL MODELLING FOR WEIGHT REDUCTION OF AIRCRAFT ENGINE HARNESS DESIGNS

TOULOUSE, FRANCE / 23 – 25 OCTOBER 2018

**BENTHEM, Roel van** <sup>(1)</sup>, **BLOEM, Edwin** <sup>(2)</sup>, **ALBERO, Franck** <sup>(3)</sup>, **AZEMARD, Laurent** <sup>(4)</sup>

<sup>(1) (2)</sup> *NETHERLANDS AEROSPACE CENTRE, NLR*  
Anthony Fokkerweg 2, 1059 CM Amsterdam  
THE NETHERLANDS  
[roel.van.benthem@nlr.nl](mailto:roel.van.benthem@nlr.nl), [edwin.bloem@nlr.nl](mailto:edwin.bloem@nlr.nl)

<sup>(2)(3)</sup> *SAFRAN ELECTRICAL & POWER*  
Parc d'activité d'Andromède, 1, rue Louis Blériot, CS 80049 31702 BLAGNAC Cedex  
FRANCE  
[franck.albero@safrangroup.com](mailto:franck.albero@safrangroup.com), [laurent.azemard@safrangroup.com](mailto:laurent.azemard@safrangroup.com)

**KEYWORDS:** flat cable, bundle, wire rating, bundle derating, harness derating, thermal modelling, weight saving, aerospace.

## ABSTRACT:

With the development of new turbofan aero engines, such as the Ultra-High Bypass Ratio (UHBR) engine and open-rotor solutions, advances in propulsion and fuel efficiency can be made through increasing fan diameters and higher bypass-ratios. This will provide less space for the engine systems and for ventilation. Moreover, higher operating temperatures are being expected. Improved technologies for the more severe conditions were investigated in the EU H2020 research project NIPSE. One of the objectives was to assess innovative flat-cable designs for extreme environmental conditions that occur in nacelles. Since flat cables have a larger cooling surface than round bundles, the derating of flat cables is expected to be less severe with respect to the recommended industrial derating in AS50881 for round bundles designs. As a consequence smaller wire gauges may be allowed in flat cables when compared to round bundles while carrying the same current, thus saving weight. To investigate this, three experimental flat cable samples (1, 2, and 3 layers of in total 22 AWG 20) have been manufactured and tested in horizontal as well as in 90 degrees rotated orientation together with references samples. The innovative derating tests, done in an altitude chamber, showed an improved performance compared to the standard AS50881 derating, demonstrating the weight saving potential of flat cables. The test results show that the derating of flat cables should be related to the number of layers. The main trend for a 1 layer flat

cable shows an increased current capability (at the same temperature differences) which can lead to a significant weight reduction up to 60%. Future investigation on use cases is required to substantiate this. Thermal modelling has been done for correlation with the derating test results and for extrapolation toward higher environmental temperature conditions up to 240°C as found in aircraft engines. The analysis indicated a model accuracy of  $\pm 5.95^\circ\text{C}$ . Future investigation to improve flat cable manufacturing methods and derating testing is recommended for optimization and use of flat cable designs by the aircraft industry in general. This will pave the way for an extension and improvement of the aerospace derating standards allowing the use of flat cables, saving weight, easing installation in narrow areas, and improving fuel economy for new aircraft.

## 1. INTRODUCTION

One of the EU/NIPSE project objectives is to optimize cable routing and to assess innovative wiring types, such as flat-cable designs, for the environmental conditions that occur in engines. The availability of state-of-the-art test facilities at NLR such as the Harness Derating Test Facility (HDTF) for evaluating of the electrical and thermal characteristics of the wiring harnesses is highly relevant for improvement of industrial manufacturing standards and maintenances processes. The HDTF (Figure 1) is a refurbished Thermal Vacuum (TV) chamber modified to control the internal pressure thus to operate as altitude chamber suitable for thermal testing of aerospace wires and harness designs.

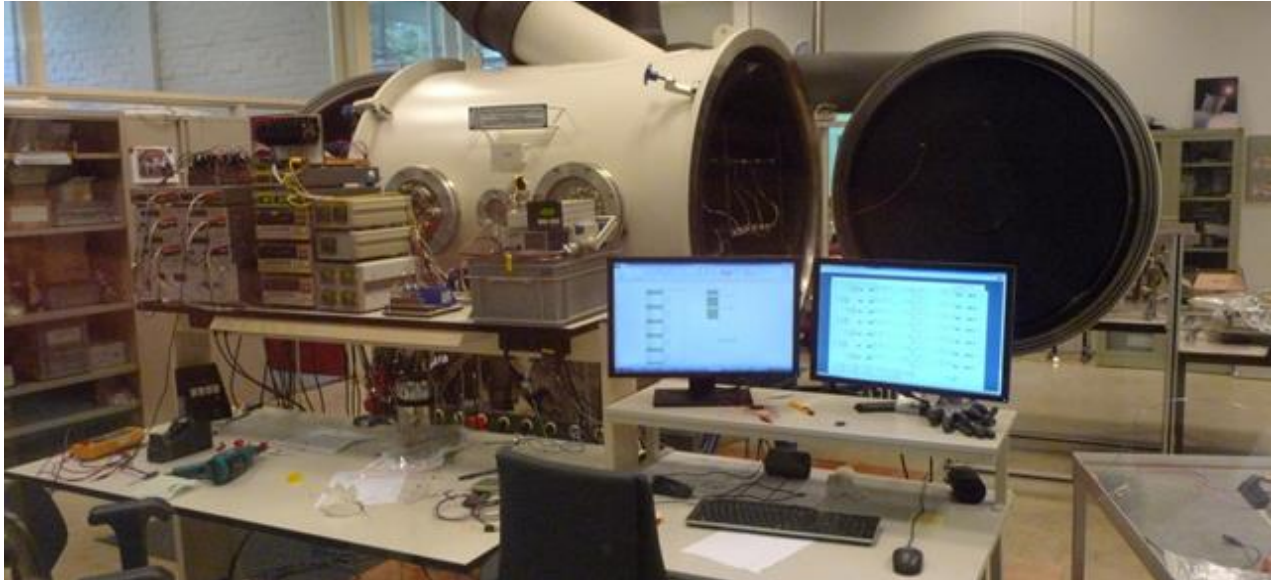


Figure 1. Harness Derating Test Facility (HDTF) at NLR

An ambitious ESA project has been conducted using the HDTF for the verification of the wire rating and bundle derating in vacuum with the aim to improve the ECSS (space) derating standards [1], [2], [3]. Derating testing of aircraft flat cables is an excellent extension of the HDTF capability for verification and improvement of the Aerospace standards when applying flat cables in aircraft systems. The test results indicated that the derating is related to the number of layers rather than the number of wires.

By the increased surface areas, natural cooling of flat cables is enhanced; the current rating of flat cables is expected to be higher with respect to round cable's allowing for higher maximum currents through a similar wire gauge, thus in theory capable to save weight.

This paper describes the flat cable samples, the test facility, the instrumentation, the test approach, test results, derating analysis and thermal modelling done for 5 samples with different wire configurations. Three flat cable samples (with 1, 2 and 3 layers respectively) and two reference samples (a single wire and a round cable) were manufactured by SAFRAN ELECTRICAL & POWER, France. The altitude tests were performed using the Harness Derating Test Facility (HDTF) of the NETHERLANDS AEROSPACE CENTRE, NLR in the Netherlands.

## 2. FLAT CABLE DERATING TESTS

The 5 samples (see Section 3.) were tested in a single run in horizontal and a single run in a 90° rotated orientation: a single wire (A) and round bundle (B) were used as reference samples, and three flat cables (C, D, E) with different layer configurations, having a similar wire size (AWG 20) and an equal number of 22 wires. At the same

currents all the samples obtain a different temperature elevation after stabilization due to equilibrium ( $Q_{in}=Q_{out}$ , i.e. Heat in = Heat out) between Joule heating ( $Q_{in}=I^2 \cdot R$ ) and natural cooling ( $Q_{out}=C \cdot \Delta T$ ). The round bundle is the hottest, the flat cables colder (related to the number of layers) and the single wire A is the coldest at the same current. The derating factors are estimated from the ratio of the currents at the same the temperature elevation of a single-wire reference sample A (Figure 2). Testing in horizontal orientation is considered worst case with respect to convective cooling.

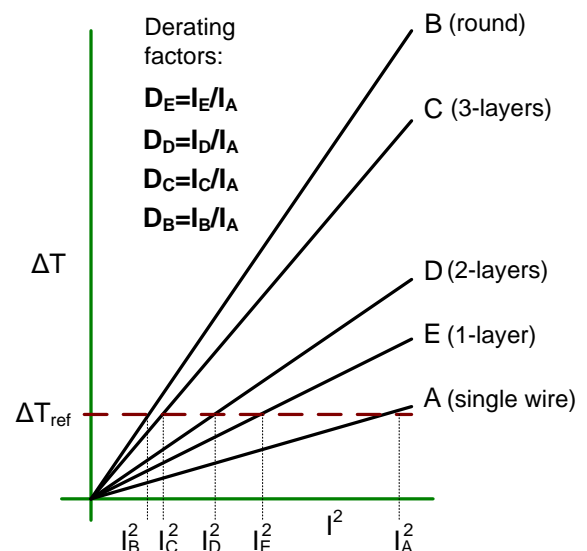


Figure 2. Temperature rise w.r.t current for the different samples at the same pressure. The derating factors are calculated by the ratio of the currents of samples B to E with respect to the current of the single wire sample, taken at a reference temperature rise (dotted line)

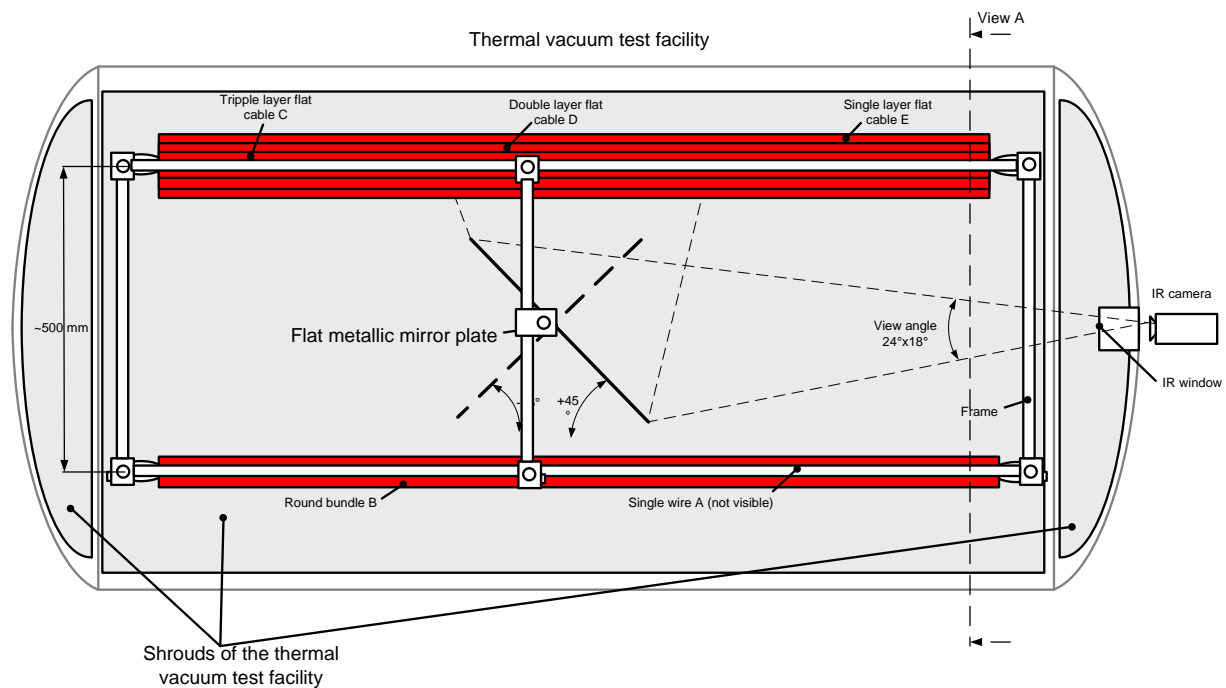


Figure 3. Harness Derating Test Facility (HDTF) for the testing an IR inspection of flat cable samples

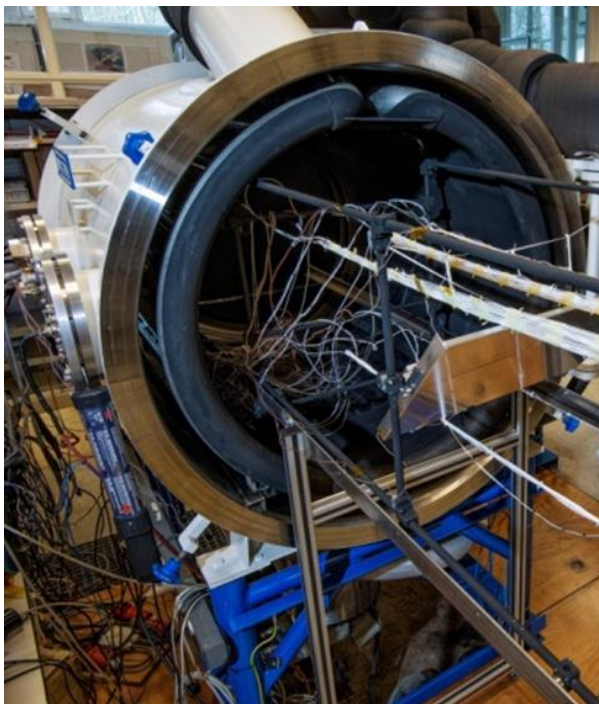


Figure 4. Harness Derating Test Facility (HDTF) at NLR prior to the flat cable testing

The cable samples were stretched in a frame which is shifted in the test facility schematically shown in Figure 3. Figure 4 shows a photograph of the setup. An IR camera system (FLIR A40) is included to visually inspect thermal gradients of the samples. The IR camera with a Field of View 18°x24° has been positioned outside the facility looking through an IR transparent window located in the centre of the facility door.

The image is projected via a +45° or -45° tilted metal plate acting as a mirror to thermally image (part) of the samples.

The highest environmental temperature tested is +100 °C. This is a limitation of the facility. For derating analysis at elevated environmental temperatures above 100°C the correlated thermal model has been extrapolated to 240°C. The thermal performance is tested at sea-level (1020mbar) and at low pressure (13 km altitude, 200mbar), which is representative for high altitude conditions and is worst case for convection. Also tests at intermediate pressures were performed. Load cases were applied by gradually increasing the current through the samples to obtain temperature steps of 25°C. The location, orientation and spacing of the samples inside the facility have been evaluated to minimize mutual convective, conductive and radiative influences.

### 3. TESTED SAMPLES

A typical wire harness is a mixture of data (passive) and power lines carrying current. However, for testing of the thermal performance, a simplified (fully) loaded harness design carrying a current is sufficient. The following guidelines were considered for definition of the sample layout. A 1 meter sample length and thermally insulated suspension is sufficient for simulation of (semi-) infinite sample lengths. A single wire size AWG 20 (EN 2267-10 A DR) is used for all samples e.g. to obtain one current group. All sample wires were electrically interconnected at both ends having extended loops, see Figure 5. This is a wire with similar size to ensure that the same current runs through all wires of each sample.



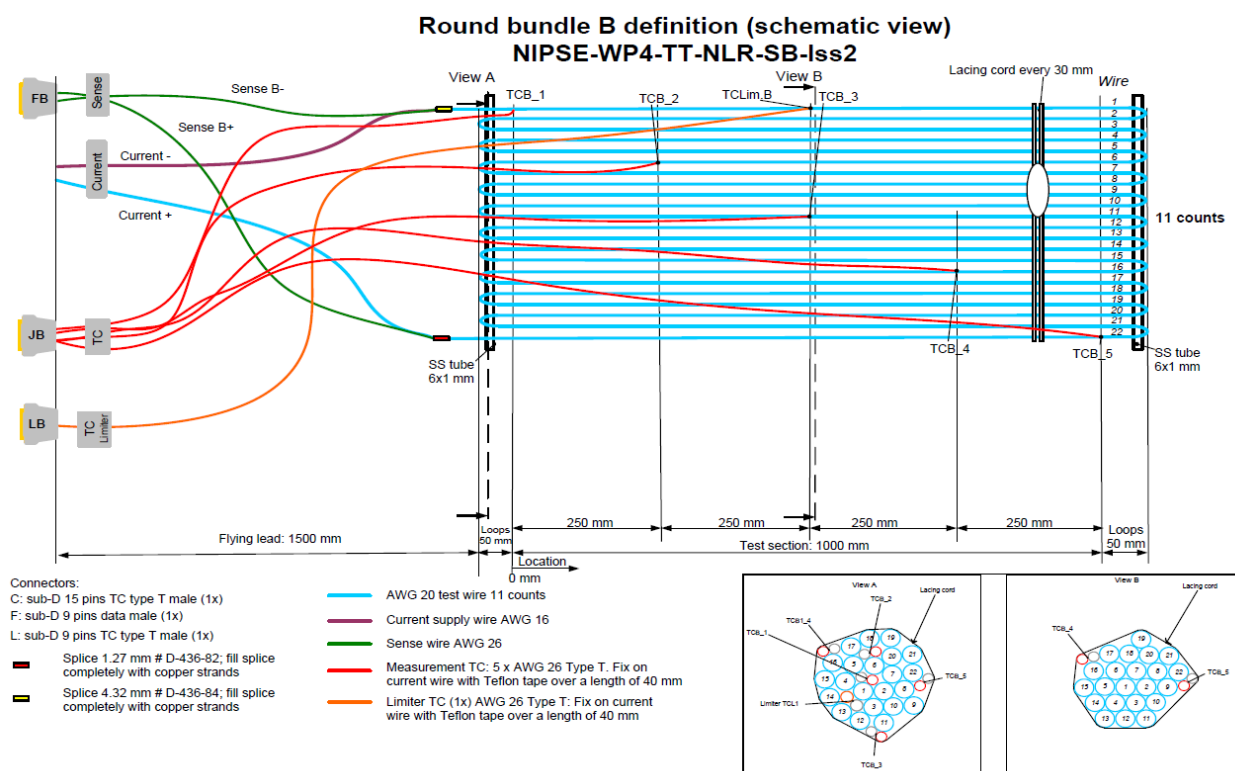



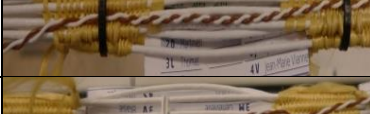



Figure 5. Example of the instrumentation of sample B

Table 1. Five samples used for thermal derating testing of Flat Cables (paper and ty-raps were removed before the test)

<b>A</b>	<b>Reference Single wire</b>	
<b>B</b>	<b>Reference: Round bundle</b>	
<b>C</b>	<b>Flat Cable 3 layers</b>	
<b>D</b>	<b>Flat Cable 2 layers</b>	
<b>E</b>	<b>Flat Cable 1 layer</b>	

The size and bending of the loops was as short as possible (ca 10cm) but the two flying leads (in and out going current lines) were extended for connection with the facility feed-through. The loops were also used to suspend the samples with stainless steel springs to compensate for

expansion by heating and to minimize conductive heat-leaks.

This arrangement allowed connecting all samples in series and using a single current source. The total length of the combined samples was 116.6 meters of wire resulting in a total resistance of nearly 4 ohm. Note that resistance and length are connected. Each sample has two sense wires measuring the voltage drop between the in- and outgoing lines to calculate the power losses for the whole sample including loops. The sense lines are thin wires with 1 to 3 meters flying leads and a connector. The length of the loops (or resistance) is subtracted from the total wire length (or resistance) for an accurate calculation of the power losses per meter sample. The current is accurately determined by measuring the voltage drop across a calibrated series shunt resistor of  $0.5 \text{ m}\Omega \pm 0.05\%$ . Each sample has additionally 3 to 6 thermocouples type T (with 1 to 3 meters flying leads) installed to monitor the temperatures. The following electrical parameters were measured for each cable bundle sample:

- Electrical current [A] is measured from the voltage drop across the shunt resistor. The same current is injected in all samples while the samples are connected in series to the same power supply;
- Voltage drop across each cable sample [V];
- Power dissipation [W] in each sample, including loops, calculated from the sensed voltage and current;
- Resistance of the cable sample [Ohm], calculated from the sensed voltage drop and current.

#### 4. TEST SEQUENCE

Flat cable specifications demonstrate endurance under high temperatures while aircraft engines run at up to 300°C external temperature. By limitations of the facility, the current rating can only be tested under non-representative (lower) ambient conditions. The maximum environmental temperature for the samples during the test is 100°C. The highest achievable pressure, to simulate sea level air, is 950mbar to ensure that the facility doors are sealed-off by a slight under-pressure with respect to the laboratory environment. A thermal model, based on physical properties, has been correlated with the test results. The validated model has been used for extrapolation towards higher (not tested) environmental temperatures. This results in a slight loss of accuracy for higher environmental temperatures. The test series T1.0 to T4.7, listed in Table 2, were conducted for both the horizontal as well as the 90° rotated orientation having a fixed shroud temperature at 100 °C. The current is increased for the hottest Sample B (round cable) increasing its temperature in steps of  $25 \pm 10^\circ\text{C}$  until a maximum of  $+240^\circ\text{C}$  is achieved. The other (cooler) samples follow, while connect in series, and the achieved temperatures are recorded after stabilization. According to AS50881 [4] the highest current for a freely suspended AWG20 wire having a temperature difference of  $140^\circ\text{C}$  (i.e.  $+240^\circ\text{C}$  in  $100^\circ\text{C}$  air) is 22 Amps in sea level air. This should be derated with a factor 0.84 at 13 km (43000 feet) altitude i.e. resulting in 18.5 Amps maximum. This will be the highest current that may occur at any point during the test. However, note that the actual current is limited by the temperature of the hottest Sample B (round cable). Sample A (single wire) has the lowest temperature any time during the test.

Table 2. Test cases and sample B target temperatures for the Flat Cable derating tests

Test Case	Pressure [Bar]	Test case	Pressure [Bar]	Target Temperature Sample B[°C]
T1.0	0.95	T3.0	0.4	~100
T1.2		T3.2		~125
T1.3		T3.3		~150
T1.4		T3.4		~175
T1.5		T3.5		~200
T1.6		T3.6		~225
T1.7		T3.7		~240
T2.0	0.7	T4.0	0.2	~100
T2.2		T4.2		~125
T2.3		T4.3		~150
T2.4		T4.4		~175
T2.5		T4.5		~200
T2.6		T4.6		~225
T2.7		T4.7		~240
The shroud temperature is 100°C for all cases				

#### 5. IR CAMERA MEASUREMENTS

An experimental IR camera system (FLIR A40) is included to thermo-visually inspect (a part of) the samples during the test.

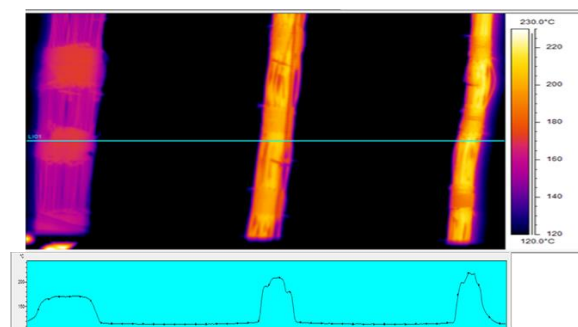


Figure 6. IR camera observation - Test case T1.6 – Cable samples E, D, C (left to right)

For temperature stabilization, the variation should be  $<1^\circ\text{C}$  per hour. Resolution of the IR camera setup is just about sufficient to resolve individual cables but this could be improved in the future. The difference in sample temperature, at the same current, is clearly visible, see Figure 6. With more layers the sample temperature increases as expected. The patches of the 1 layer sample (E) have a slightly higher temperature ( $\pm 5\text{--}10^\circ\text{C}$ ) than the individual cables. This can be related to a slightly poorer cooling to air at the location of the patches. A slight thermal gradient is visible towards the edges of the flat cable samples but this could also be related to the resolution of the IR camera system.

#### 6. TEMPERATURE MEASUREMENTS

Temperature differences between thermocouples (TCs) within the same cable bundle were observed, up to  $52^\circ\text{C}$  (for round cable sample B) and up to  $43^\circ\text{C}$  (for flat cable samples), depending on the current and ambient pressure. These temperature gradients are caused by:

- location of the TCs in axial direction in the bundle,
- location of the TCs in radial direction in the bundle,
- mounting of the TCs to the cable wires.

For derating analysis the maximum measured temperature in each bundle is used instead of the average, as a worst-case value. Figure 7 shows the  $\Delta T$  graphs for the horizontal and Figure 8 the 90 degrees rotated orientation, both in ambient and low pressure in a  $100^\circ\text{C}$  environment.

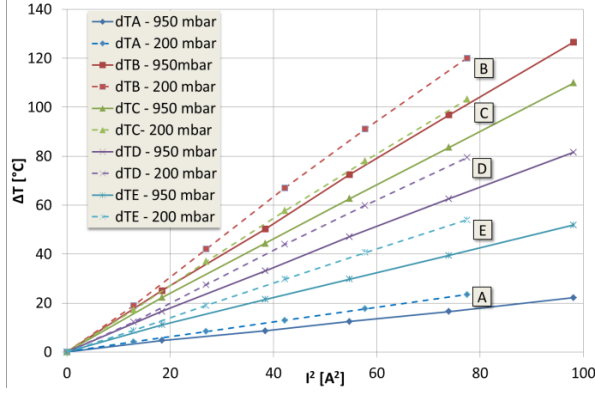


Figure 7. Maximum measured temperature rise above 100°C at a minimum pressure (200 mbar) and a maximum pressure (950 mbar) as function of the square of the current for samples in horizontal orientation

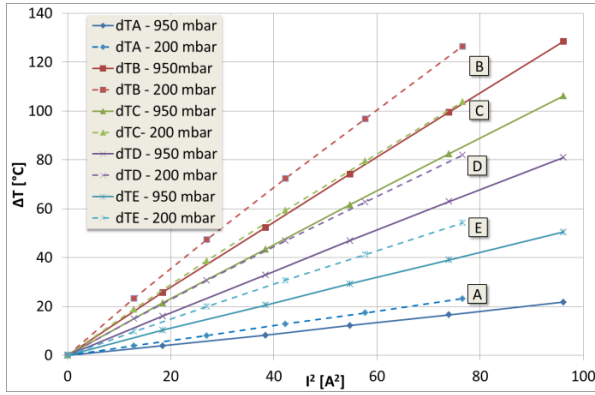


Figure 8. Maximum measured temperature rise above 100°C at a minimum pressure (200 mbar) and a maximum pressure (950 mbar) as function of the square of the current for samples in 90 degrees rotated orientation.

## 7. DERATING EVALUATION APPROACH

Given the temperature rating of a wire and the temperature of the ambient air, the corresponding free-wire-sea-level-air current rating, in this paper referred to as “standard current rating,” can be determined according to the SA50881 standard [4]. Since increased altitude yields reduced air pressure, which yields reduced convective cooling capacity, the sea-level current rating is too optimistic at increased altitudes (lower air pressure) and needs to be “de-rated” by applying an “altitude derating factor”  $d_h^{\text{alt}} \leq 1$  for altitude  $h$ , or a “pressure derating factor”  $d_p^{\text{press}} \leq 1$  for pressure  $p$  to guarantee that the wire temperature stays below its temperature rating. In this paper we will use the pressure derating factor  $d_p^{\text{press}}$ . Bundling multiple wires together makes convective and radiative cooling less effective. This means that also for wire bundles, the standard current rating is too optimistic and needs to be de-rated by applying a “bundle derating factor”  $d_X^{\text{bundle}} < 1$  for bundle  $X$  to

guarantee that the temperatures of the wires in bundle  $X$  stay below their temperature rating. Taking into account both the pressure (or altitude) as well as the bundle configuration, the “effective current derating factor”  $d_{X,p}^{\text{eff}} \leq 1$  for bundle  $X$  at pressure  $p$  is given by the product of the bundle derating factor and the pressure derating factor under the assumption that they are fully independent factors:

$$d_{X,p}^{\text{eff}} = d_X^{\text{bundle}} \times d_p^{\text{press}} \quad (\text{Eq. 1})$$

Let  $I_{X,p,\Delta T}$  denote the current applied to bundle sample  $X$ ,  $X \in \{A, B, C, D, E\}$  at pressure  $p$  that yields a temperature rise of  $\Delta T$  above ambient temperature. Notice that sample  $A$  is a single-wire sample.

By virtue of the derating standard, the current flowing through a bundle  $X$  of wires, yielding a temperature rise  $\Delta T$  at pressure  $p$ , is proportional to the product of the current flowing through a single wire (of the same type as the wires in the bundle) yielding the same temperature rise  $\Delta T$  at the same pressure  $p$  and the bundle derating factor  $d_X^{\text{bundle}}$ :

$$I_{X,p,\Delta T} = I_{A,p,\Delta T} \times d_X^{\text{bundle}} \quad (\text{Eq. 2})$$

Also by virtue of the derating standard, the current flowing through a bundle  $X$  of wires, yielding a temperature rise  $\Delta T$  at pressure  $p$ , is proportional to the product of the current flowing through the same bundle  $X$  yielding the same temperature rise  $\Delta T$  at sea-level pressure and the pressure derating factor  $d_p^{\text{press}}$ :

$$I_{X,p,\Delta T} = I_{X,950,\Delta T} \times d_p^{\text{press}} \quad (\text{Eq. 3})$$

Since the bundle derating factor  $d_X^{\text{bundle}}$  is by definition assumed to be independent of the pressure, it follows that measurements for  $d_X^{\text{bundle}}$  can be obtained at any pressure  $p$ . Thus from (Eq. 2) it follows that

$$d_X^{\text{bundle}} = \frac{I_{X,p,\Delta T}}{I_{A,p,\Delta T}} \quad (\text{Eq. 4})$$

is a measurement for  $d_X^{\text{bundle}}$  irrespective of the pressure  $p$ . With the measurements  $d_{X,p}^{\text{bundle}}$ , an estimate of  $d_X^{\text{bundle}}$  can be obtained by taking the average of the measurements over all pressures  $p \in \{200, 400, 700, 950\}$ .

Since the pressure derating factor  $d_p^{\text{press}}$  is by definition assumed to be independent of the

bundle configuration, it follows that measurements for  $d_p^{\text{press}}$  can be obtained from any bundle configuration  $X$ . Thus from (Eq. 3) it follows that

$$d_{X,p}^{\text{press}} = \frac{I_{X,p,\Delta T}}{I_{X,950,\Delta T}} \quad (\text{Eq. 5})$$

is a measurement for  $d_p^{\text{press}}$  irrespective of the bundle configuration  $X$ . With the measurements  $d_{X,p}^{\text{press}}$  an estimate of  $d_p^{\text{press}}$  can be obtained by taking the average of the measurements over all bundle configurations  $X \in \{A,B,C,D,E\}$ .

## 8. DERATING RESULTS

Following our derating approach presented in section 7, from the measurement results the cable bundle derating was determined for the horizontal and 90° rotated orientation. To this end, a reference temperature difference  $\Delta T_{\text{ref}}$  of 20°C was used and for each sample the current ( $I_{X,p,\Delta T}$ ,  $X \in \{A,B,C,D,E\}$ ,  $p \in \{200,400,700,950\}$ ) at  $\Delta T=20^\circ\text{C}$  is calculated from the best-straight-line through the measurements.

Table 3. Derating factors in horizontal and 90 degrees rotated orientation showing a marginal difference.

HORIZONTAL					
$d_{X,p}^{\text{eff}} = d_X^{\text{bundle}} \times d_p^{\text{press}}$					
	pressure	950	700	400	200
bundle	$d_X^{\text{bundle}} \backslash d_p^{\text{press}}$	1.000	0.984	0.944	0.909
A	1.000	1.000	0.984	0.944	0.909
B	0.376	0.376	0.370	0.355	0.342
C	0.426	0.426	0.419	0.402	0.387
D	0.473	0.473	0.465	0.447	0.430
E	0.583	0.583	0.574	0.550	0.530

90 degrees rotated					
$d_{X,p}^{\text{eff}} = d_X^{\text{bundle}} \times d_p^{\text{press}}$					
	pressure	950	700	400	200
bundle	$d_X^{\text{bundle}} \backslash d_p^{\text{press}}$	1.000	0.976	0.929	0.882
A	1.000	1.000	0.976	0.929	0.882
B	0.376	0.376	0.367	0.349	0.332
C	0.419	0.419	0.409	0.389	0.370
D	0.466	0.466	0.455	0.433	0.411
E	0.578	0.578	0.564	0.537	0.510

A summary of the estimated derating factors is presented in Table 3 showing a marginal difference between the horizontal and rotated orientation. In Table 4 and Table 5 an overview of all derating results is presented. For verification, Table 4 and Table 5 also show the results for the estimated effective derating  $d_{X,p}^{\text{eff}} = d_X^{\text{bundle}} \times d_p^{\text{press}}$  and the measured total derating  $I_{X,p,\Delta T} / I_{A,950,\Delta T}$  at  $\Delta T=20^\circ\text{C}$ . As expected the estimated effective derating and the measured total derating closely match each other.

The measurements confirm our derating approach, when comparing bundle temperatures at the same currents and at different pressures. According to SA50881 [4] the derating increases (lower numbers) with reduced air pressures, which we also measured during the tests, however with a small margin. See also Figure 9. When the pressure derating with respect to altitude is included the weight benefit improves. The flat cable derating factor (Figure 10) shows a significant margin with respect to the 100% load case for a round cable.

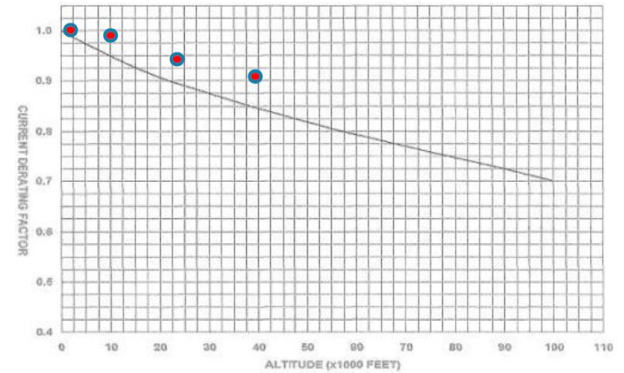


Figure 9. Averaged pressure derating of all samples compared with AS 50881 showing a margin.

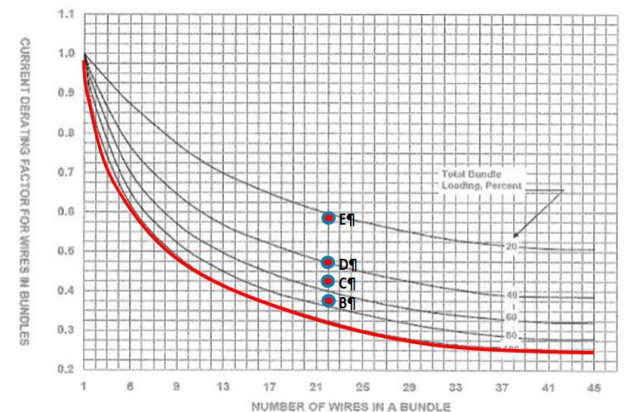


Figure 10. Averaged bundle derating of the 100% loaded 22 wires flat cable samples B,C,D,E with respect to a round bundle, 100% loaded (red line) (ref AS 50881)) showing a significant derating margin.



Table 4: Derating test results for the horizontal orientation

HORIZONTAL						
		$I_{X,p,\Delta T} \text{ , } \Delta T=20^{\circ}\text{C}$				
$\begin{matrix} \text{p} \\ \text{X} \end{matrix}$	950 mbar	700 mbar	400 mbar	200 mbar		
A	9.42	9.09	8.65	8.08		
B	3.45	3.38	3.25	3.16		
C	3.84	3.85	3.71	3.58		
D	4.30	4.24	4.08	4.01		
E	5.34	5.27	5.04	4.85		
		$d_{X,p}^{\text{bundle}} = I_{X,p,\Delta T} / I_{A,p,\Delta T} \text{ , } \Delta T=20^{\circ}\text{C}$				$d_X^{\text{bundle}}$
$\begin{matrix} \text{p} \\ \text{X} \end{matrix}$	950 mbar	700 mbar	400 mbar	200 mbar		
A	1	1	1	1	1.000	
B	0.366	0.372	0.376	0.391	0.376	
C	0.408	0.424	0.430	0.443	0.426	
D	0.457	0.466	0.472	0.496	0.473	
E	0.567	0.580	0.582	0.600	0.583	
		$d_{X,p}^{\text{press}} = I_{X,p,\Delta T} / I_{X,950,\Delta T} \text{ , } \Delta T=20^{\circ}\text{C}$				
$\begin{matrix} \text{p} \\ \text{X} \end{matrix}$	950 mbar	700 mbar	400 mbar	200 mbar		
A	1	0.965	0.918	0.858		
B	1	0.980	0.944	0.916		
C	1	1.002	0.967	0.932		
D	1	0.986	0.950	0.932		
E	1	0.987	0.942	0.908		
$d_p^{\text{press}}$	1	0.984	0.944	0.909		
		$d_{X,p}^{\text{eff}} = d_X^{\text{bundle}} \times d_p^{\text{press}}$				
$\begin{matrix} \text{p} \\ \text{X} \end{matrix}$	950 mbar	700 mbar	400 mbar	200 mbar		
A	1.000	0.984	0.944	0.909		
B	0.376	0.370	0.355	0.342		
C	0.426	0.419	0.402	0.387		
D	0.473	0.465	0.447	0.430		
E	0.583	0.574	0.550	0.530		
		$I_{X,p,\Delta T} / I_{A,950,\Delta T} \text{ , } \Delta T=20^{\circ}\text{C}$				
$\begin{matrix} \text{p} \\ \text{X} \end{matrix}$	950 mbar	700 mbar	400 mbar	200 mbar		
A	1.000	0.965	0.918	0.858		
B	0.366	0.359	0.345	0.336		
C	0.408	0.409	0.394	0.380		
D	0.457	0.450	0.433	0.426		
E	0.567	0.559	0.535	0.515		

Table 5: Derating test results for the 90 degrees rotated orientation

90 degrees rotated					
	$I_{X,p,\Delta T}$ , $\Delta T=20^{\circ}\text{C}$				
$\begin{matrix} p \\ X \end{matrix}$	950 mbar	700 mbar	400 mbar	200 mbar	
A	9.42	9.25	8.75	8.12	
B	3.43	3.35	3.20	3.06	
C	3.91	3.81	3.65	3.51	
D	4.39	4.26	4.04	3.86	
E	5.44	5.29	5.02	4.77	
	$d_{X,p}^{\text{bundle}} = I_{X,p,\Delta T} / I_{A,p,\Delta T}$ , $\Delta T=20^{\circ}\text{C}$				$d_X^{\text{bundle}}$
$\begin{matrix} p \\ X \end{matrix}$	950 mbar	700 mbar	400 mbar	200 mbar	
A	1	1	1	1	
B	0.364	0.362	0.366	0.376	
C	0.415	0.412	0.418	0.432	
D	0.466	0.460	0.462	0.475	
E	0.578	0.572	0.574	0.587	
	$d_{X,p}^{\text{press}} = I_{X,p,\Delta T} / I_{X,950,\Delta T}$ , $\Delta T=20^{\circ}\text{C}$				
$\begin{matrix} p \\ X \end{matrix}$	950 mbar	700 mbar	400 mbar	200 mbar	
A	1	0.982	0.929	0.862	
B	1	0.976	0.935	0.892	
C	1	0.976	0.935	0.899	
D	1	0.971	0.922	0.880	
E	1	0.973	0.923	0.876	
$d_p^{\text{press}}$	1	0.976	0.929	0.882	
	$d_{X,p}^{\text{eff}} = d_X^{\text{bundle}} \times d_p^{\text{press}}$				
$\begin{matrix} p \\ X \end{matrix}$	950 mbar	700 mbar	400 mbar	200 mbar	
A	1.000	0.976	0.929	0.882	
B	0.376	0.367	0.349	0.332	
C	0.419	0.409	0.389	0.370	
D	0.466	0.455	0.433	0.411	
E	0.578	0.564	0.537	0.510	
	$I_{X,p,\Delta T} / I_{A,950,\Delta T}$ , $\Delta T=20^{\circ}\text{C}$				
$\begin{matrix} p \\ X \end{matrix}$	950 mbar	700 mbar	400 mbar	200 mbar	
A	1.000	0.982	0.929	0.862	
B	0.364	0.356	0.340	0.325	
C	0.415	0.405	0.388	0.373	
D	0.466	0.452	0.429	0.410	
E	0.578	0.562	0.533	0.506	



## 9. THERMAL MODELING

All samples have been modelled to fit within a rectangle box including the single wire, see Figure 11. The power  $P_i$  [W] dissipated by wire  $i$  is given by

$$P_i = I_i^2 R_i \quad (\text{Eq. 6})$$

where  $P_i$  [W] is the power (electrical energy per unit time in Watt) converted from electrical energy to thermal energy,  $R_i$  [Ohm] is the resistance of the conductor in Ohm, and  $I_i$  [A] is the current through wire  $i$  in Ampère.

The resistance of the conductor of wire  $i$  depends on the conductor temperature  $T_{c,i}$  [K], the conductor reference resistance  $R_{\text{ref},i}$  [Ohm/m] at reference temperature  $T_{\text{ref},i}$  [°C], the conductor temperature coefficient of resistance  $\alpha_{R,i}$  [1/K], and the conductor length  $L$  [m]:

$$\begin{aligned} R(T_{c,i}) &= R(R_{\text{ref},i}, \alpha_{R,i}, T_{\text{ref},i}, T_{c,i}, L) \\ &= L \cdot R_{\text{ref},i} \left( 1 + \alpha_{R,i} ((T_{c,i} - 272.15) - T_{\text{ref},i}) \right) \end{aligned} \quad (\text{Eq. 7})$$

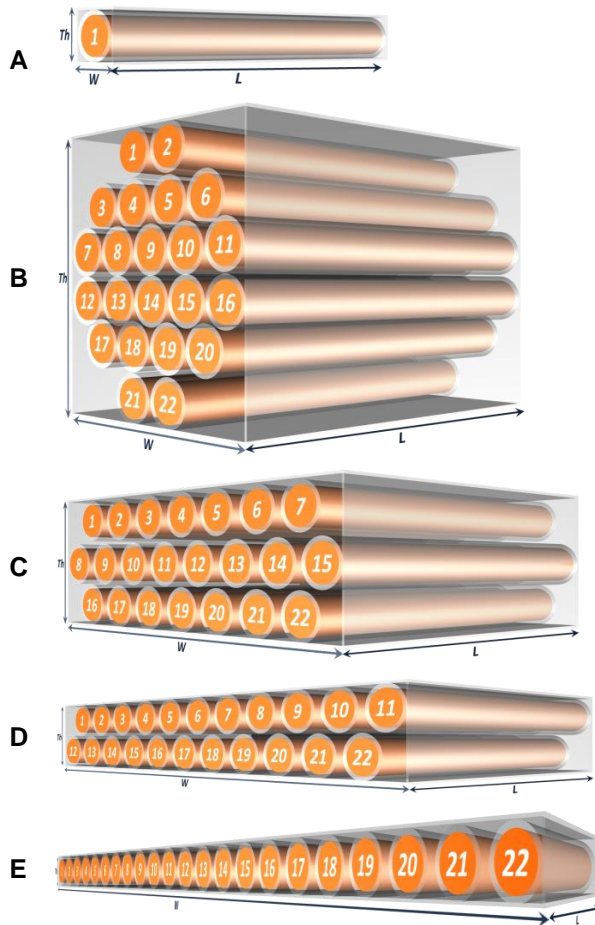


Figure 11. Thermal models of the tested samples considering a rectangular box for convection.

The thermal system of two arbitrary wires inside a flat cable with their corresponding heat transfers can be modelled by a thermal network defined by a set of nodes and conductance's (thermal couplings), see Figure 12.

Note that the centre of each wire is taken to produce the worst case temperature. The statistics shows a good model correlation (Table 6) with the laboratory measurements. In particular for the single wire the correlation results in a maximum difference of  $\pm 1.61^\circ\text{C}$  between the predictions and the laboratory measurements. The overall maximum difference of  $\pm 5.95^\circ\text{C}$  between the predictions and the laboratory measurements is obtained for the 2-layers cable for the horizontal case.

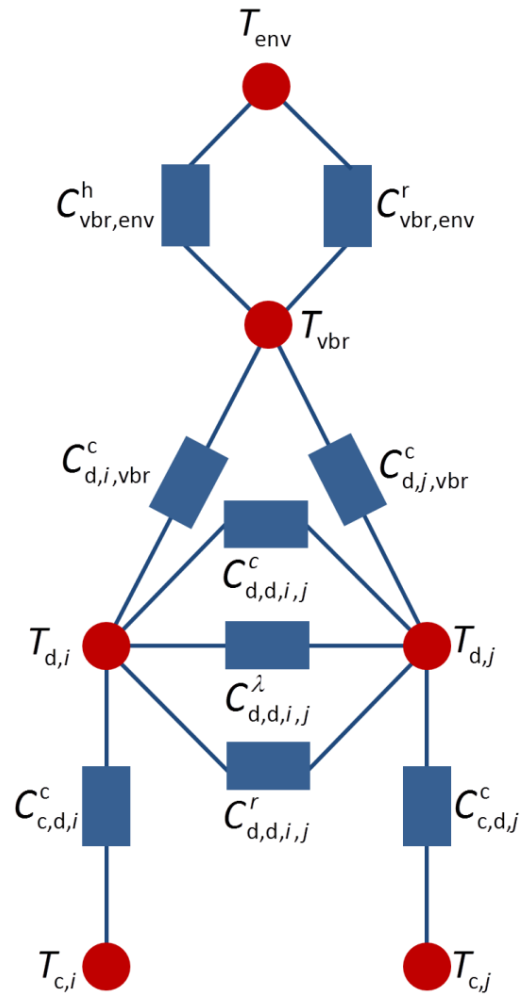


Figure 12. Thermal network of nodes and conductors (thermal couplings) for two arbitrary wires inside a flat cable. The unit of the nodes temperatures (red circles) are [°C] and the thermal couplings (blue rectangles) are indicated by [W/°C]. In the subscripts, c indicates conductor, d indicates dielectric insulation, vbr indicates virtual braid and env indicates environment. In the superscripts c indicates contact conduction,  $\lambda$  indicates air conduction, h indicates convection, and r indicates radiation.

Table 6. Statistical difference between the predicted and measured cable temperature for the horizontal and 90 degrees rotated case.

Horizontal Case					
	A Single Wire	B Round	C 3 Layers	D 2 layers	E 1 layer
$ \Delta T $ Min	0.00	0.47	0.57	0.09	0.25
$ \Delta T $ Max	1.44	3.20	4.12	5.95	4.12
$\Delta T$ Mean	0.62	1.00	1.28	-0.72	1.10
$\Delta T$ St dev	0.35	1.50	2.39	2.80	2.04

90° Rotated Case					
	A Single Wire	B Round	C 3 Layers	D 2 layers	E 1 layer
$ \Delta T $ Min	0.03	0.90	1.20	1.56	0.81
$ \Delta T $ Max	1.61	4.57	5.31	4.65	4.70
$\Delta T$ Mean	0.22	2.67	3.92	3.50	3.07
$\Delta T$ St dev	0.40	1.06	1.27	0.89	1.05

## 10. CONCLUSIONS & RECOMMENDATIONS

The development of an innovative derating test facility demonstrated an improved performance of horizontal and rotated flat cable samples with respect to the reference samples (a single wire and round cable) and with respect to the aerospace derating standard AS50881 [4]

- The flat cable and reference samples were manufactured and instrumented by SAFRAN.
- The flat cables were tested in NLR Harness Derating Test Facility at NLR
- Introduction of IR camera proved to be a valuable tool for improved understanding of the test results
- The derating of flat cables can be related to the number of layers.
- For a 1 layer Flat Cable up to a 1.8 times higher current was found in ambient air which leads to a theoretical weight reduction of 60%.
- The single wire and round bundle test results show that AS50881 includes a conservative margin of 15%. The performances of flat harness compared to AS50881 include this margin.
- An update of the aerospace derating standards to promote the use of flat harnesses designs is recommended.
- Thermal modelling has been done for correlation with the test results (in a 100°C environment). The analysis shows a model accuracy of  $\pm 5.95$  °C for all samples.
- Extrapolation toward higher environmental temperature conditions at 200°C shows a marginal difference of the derating factors. This demonstrates that tests done at 100°C can be considered as a good reference case for derating analysis.

The innovative derating test demonstrated an improved performance of horizontal and rotated flat cable samples with respect to the reference samples (a single wire and round cable) and with respect to the SAE50881. The derating of flat cables should be related to the number of layers. A marginal difference in derating between the horizontal and rotated samples is found. For a 1 layer Flat Cable up to a 1.8 times higher allowed current was found in ambient air which leads to a theoretical potential weight reduction of approximately 60%. The estimated weight improvement is also valid for altitude/low pressure conditions. It should be verified with use cases how much of the predicted mass reduction is achievable in practice.

## 11. ACKNOWLEDGEMENTS

The above research has been done as part of the NIPSE (Novel Integration of Powerplant System Equipment) project. This project ([www.nipse.eu](http://www.nipse.eu)) has received funding from the European Union's Horizon 2020 research and innovation program under Grant Agreement N° 636218.

## 12. ABBREVIATIONS AND ACRONYMS

HDTF	Harness Derating Test Facility
NLR	Netherlands Aerospace Centre
SEP	Safran Electric & Power
TC	Thermocouple

## 13. REFERENCES

1. Roel van Benthem, Wubbo de Grave, and Fennanda Doctor, Simon Taylor, Kees Nuyten, Pierre-Alexis Jacques Dit Routier, *Thermal analysis of wiring bundles for weight reduction and improved safety*, AIAA 2011-5111, 41st International Conference on Environmental Systems (ICES), 17 - 21 July 2011, Portland, Oregon, USA,
2. Benthem, R.C. van; Doctor, F.; Malagoli, M; Bonnafous, B, *Derating Standards and Thermal Modelling Tools for Space Harness Designs*, 45th International Conference on Environmental Systems (ICES), 12-16 July 2015, Bellevue, Washington, Seattle, USA ,
3. Marc Malagoli, Yoann, Allewaert , Roel C. van Benthem , Wubbo de Grave , Adry van Vliet, Denis Lacombe , Leo Farhat, *Improvement of the Wire Rating Standards based on TV Testing and Thermal Modeling*, 48th International Conference on Environmental Systems, ICES-2018-162, 8-12 July 2018, Albuquerque, New Mexico.
4. Aerospace Standard, Wiring Aerospace Vehicle, AS50881.



**NLR**

Anthony Fokkerweg 2  
1059 CM Amsterdam, The Netherlands  
p ) +31 88 511 3113  
e ) [info@nlr.nl](mailto:info@nlr.nl) i ) [www.nlr.nl](http://www.nlr.nl)